

# MODIS detector differences using deep convective clouds and desert targets

Qiaozhen Mu<sup>1</sup>, Amit Angal<sup>1</sup>, Kevin Twedt<sup>1</sup>, Aisheng Wu<sup>1</sup>, Xiaoxiong Xiong<sup>2</sup>

<sup>1</sup> Science Systems and Applications, Inc, 10210 Greenbelt Road, Lanham, MD 20706.

<sup>2</sup> Sciences and Exploration Directorate, NASA/GSFC, Greenbelt, MD 20771.

**Abstract:** An accurate on-orbit characterization of the Moderate Resolution Imaging Spectroradiometer (MODIS) sensors onboard the Terra and Aqua satellites is essential to satisfy the requirements from the scientific community for high-quality operational and research products. In this study, NASA's C6.1 L1B data are utilized to assess the stability of the calibrated top of atmosphere reflectance retrieved from individual detectors within a spectral band over deep convective clouds (DCCs) and desert sites. The results from these invariant Earth targets show detector-to-detector (D2D) differences in the L1B reflectance products for select MODIS reflective solar bands. For Aqua MODIS, the D2D differences have no significant change over time for the bands studied. However, the D2D differences exhibit an increase in magnitude over time for Terra MODIS bands 1, 3-7, and 26, which can induce noticeable striping and higher uncertainties in the downstream data products. The D2D stability assessment results over DCCs are consistent with those observed over desert sites. In addition, the view-angle dependence of the D2D differences is investigated by separating the frames along scan into five zones. The D2D assessment is performed for each of the five zones, and the results will further benefit any improvements in the calibration of a detector-dependent response versus scan angle that can be considered for future MODIS Level 1B Collections.

**Keywords:** MODIS, detector-to-detector difference, L1B reflectance product, response versus scan angle (RVS), deep convective clouds (DCCs)

## 1. Introduction and Motivation

The Moderate Resolution Imaging Spectroradiometer (MODIS) sensors onboard the Terra and Aqua satellites have 20 reflective solar bands (RSBs) covering wavelengths from 0.4 to 2.1  $\mu\text{m}$ , supporting numerous land, ocean, and atmospheric studies<sup>1</sup>. Terra and Aqua MODIS have been in operation for more than 20 and 18 years, respectively, far beyond their designed life of six years. As the instruments continue to age, significant degradation of the instrument gain is observed, particularly at short wavelengths.

As the MODIS scan mirror rotates, each side scans its onboard calibrators as well as the Earth view (EV) port. The reflectivity of each side of the scan mirror is a function of the angle of incidence (AOI), known as the sensor's response versus scan angle (RVS) function. The individual detectors of the RSBs are primarily calibrated on-orbit using the onboard calibration sources, such as a solar diffuser (SD) with a known prelaunch bidirectional reflectance factor (BRF) and a SD stability monitor (SDSM)<sup>1-2</sup>, as well as near-monthly lunar measurements acquired from the instrument's space-view port<sup>3</sup>. The specified uncertainty for RSBs at the typical scene level between the scan angles of  $\pm 45^\circ$  is 2% in reflectance and 5% in radiance<sup>1</sup>. The instrument's calibration coefficient,  $m_1$ , is derived from regular SD calibration measurements. Together, the SD and lunar measurements are utilized to estimate the on-orbit changes in RVS. For Terra bands 1-4, 8-10, and Aqua bands 1-4, 8-9, response trends from pseudo-invariant desert sites are supplemented to the onboard measurements to track RVS. For the Short-Wave Infrared (SWIR) bands, no noticeable on-orbit changes in the RVS have been observed. In the current Collection

6.1 calibration algorithm, an additional correction derived using Earth scene measurements is implemented for select short wavelength RSBs, namely Terra bands 3, 8-12 and Aqua bands 8-12, to account for the residual detector-to-detector biases observed in the SD-derived gain<sup>5</sup>. Uncertainties associated with the SD calibration may manifest in the calibrated L1B products as detector striping, an undesirable feature for higher level science products.

Stability assessments of the MODIS L1B reflectance products over time, between different detectors, and at different AOIs are important methods to evaluate the performance of the MODIS RSB calibrations. When evaluating the performance of the calibration, some investigations have found detector striping in the L1B images<sup>6-9</sup>. Mu et al.<sup>10</sup> evaluated the detector-to-detector differences (D2D differences) for SNPP VIIRS and found them to exhibit an increase in magnitude over time, especially for the VIS/NIR bands over deep convective clouds (DCCs) and at desert sites. DCCs are bright, natural Earth targets in the tropics, located at the tropopause level, where effects of atmospheric absorption are negligible, and can be easily identified using an  $\sim 11\text{-}\mu\text{m}$  band brightness temperature threshold of 205 K<sup>11-12</sup>. DCCs can be treated as solar diffusers that have predictable and near Lambertian albedos with high signal to noise ratio (SNR)<sup>11</sup>. The purpose of this study is to investigate whether the D2D differences still exist post-calibration, as well as to examine their temporal changes in Terra and Aqua MODIS L1B reflectance products using DCCs for RSBs 1, 3-7, and 26. In addition, the view-angle dependence of the D2D is investigated by separating the frames along scan into five zones. Other MODIS RSB bands saturate while viewing DCCs and are therefore not considered in this analysis. The results over DCCs are compared with those obtained from a desert site, and results indicate consistent trends between the two sources.

## 2. Methodology and Background

The 1-km aggregated MOD021KM (Terra) and MYD021KM (Aqua) C6.1 NASA L1B data over the eastern Indian and western Pacific Oceans (30°S-30°N and 95°E-175°E) are collected to investigate the D2D differences using the DCC technique. Due to the instrument configuration switches at mission beginning for Terra, this study focuses on data collected from July 2002 to April 2020 for both Terra and Aqua. Monthly MODIS DCC samples are divided into five frame zones (Z1-Z5) as shown in Table 1. The frame number in each L1B granule is related to the AOI by Equation 1,

$$AOI = \frac{65.5^\circ - 105^\circ}{1353} \cdot F + 10.5^\circ, \quad (1)$$

where  $F$  is the frame number. The focus of this study is at nadir in Z3 with frame numbers ranging from 571 to 840. In each frame zone, the DCC samples are further grouped according to the 10 detectors. Doelling et al.<sup>13</sup> found that the mode statistic is superior to the mean statistic when there are more than one million DCC samples, and the probability distribution functions (PDFs) are smooth. Figure 1 shows example monthly PDFs of DCC reflectance for the 10 detectors of band 1 in April 2020 for both Terra and Aqua MODIS. The number of DCC samples for each detector is less than one million, and the curves are not smooth enough to obtain reliable modes corresponding to the peaks of the PDFs. The shape of the PDF, number of pixels, and noise in the curve are generally consistent throughout the mission. In this study, the monthly mean reflectance over all the DCCs for any given detector is used instead of the mode reflectance to explore the D2D differences over time.

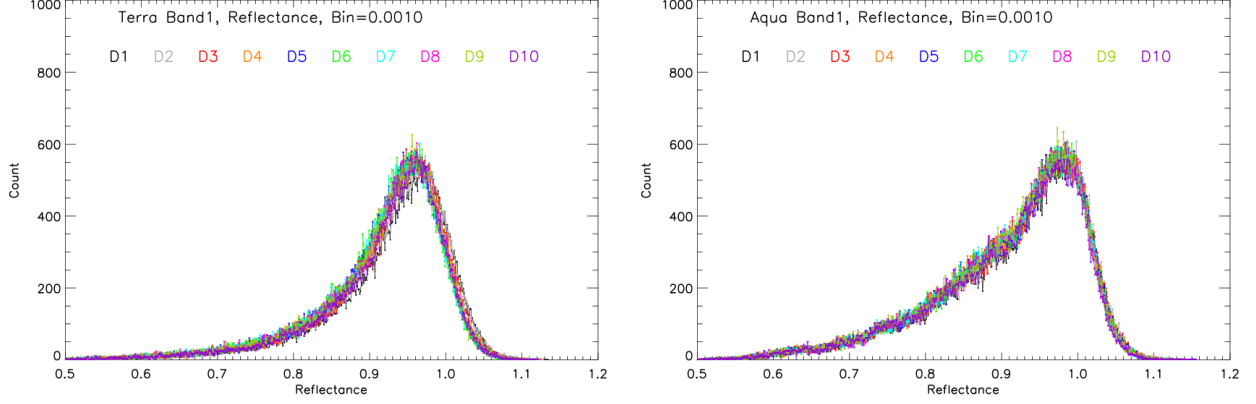


**Figure 1** Probability distribution functions (PDFs) of reflectance over DCCs using nadir frames for the 10 detectors of Terra and Aqua band 1 in April 2020.

**Table 1** The five frames zones with frame number ranges, center frames and AOIs corresponding to the center frames along each scan.

Zones	1	2	3	4	5
Frame Range	1–270	271–540	541–810	811–1080	1081–1354
Center Frame	136	406	676	946	1218
Center AOI (°)	16.0	27.0	38.0	49.0	60.0

In the MODIS L1B reflectance product, the EV reflectance factor,  $\rho_{EV} \cdot \cos(\theta_{EV})$ , is generated using the  $m_1$  and RVS Look-Up-Tables (LUTs), as well as the background and instrument temperature corrected EV digital numbers,  $dn_{EV}^*$ , as in Equation 2:

$$\rho_{EV} \cdot \cos(\theta_{EV}) = (m_1/RVS) \cdot dn_{EV}^* \cdot (d_{ES\_EV})^2, \quad (2)$$

where the  $\theta_{EV}$  is the solar zenith angle of the EV frame, and  $d_{ES\_EV}$  is the Earth–Sun distance (in AU) at the time of the EV observation<sup>4</sup>. The  $m_1/RVS$  represents the inverse of the instrument gain at any scan-angle and is detector, mirror side, sub-frame, and band-dependent. The C6.1 L1B product can have some uncertainties associated with the forward prediction of the calibration LUTs ( $m_1$  and RVS) that are updated periodically. In addition, adjustments made to the C6.1 calibration algorithm to account for the degrading sensor behavior can also lead to changes in the reflectance trending. This is especially true for recent updates made in a crosstalk correction algorithm used to calibrate the Terra SWIR bands<sup>14</sup>. To avoid the impact of these effects on the D2D difference assessment, we instead use the reflectance derived from an entire mission reprocessed set of  $m_1$  and RVS LUTs using a consistent algorithm. Since the RSB calibration equation is linear, the C6.1 L1B reflectance is easily converted to a reprocessed reflectance using a simple ratio between the two LUTs. The resulting reflectance values trend smoothly over the mission and represent the expected values that would be present in the next collection of MODIS LUTs using the best available algorithm. The D2D differences are calculated as the ratios of detector mean reflectances to the band averaged reflectances for bands 1, 3-7, and 26. Since Aqua band 6 has noisy and inoperable detectors, it is not considered in this analysis.

Studies have shown that the reflectance corrected by the bidirectional reflectance distribution function (BRDF) coefficients works better for VIS and NIR RSBs in comparison with the SWIR bands<sup>12,15</sup>. In this study, the monthly BRDF-corrected reflectances over all the DCC samples are used to derive the PDFs and the mean reflectance for each detector in Terra and Aqua MODIS B1, B3, and B4. For the SWIR bands, the original reflectance is used with no BRDF correction. For simplification, BRDF-corrected reflectance for bands 1, 3, and 4 and non-BRDF-corrected reflectance for SWIR bands will be referred to as reflectance in this study. Figure 1 shows obvious differences in the PDF curves and reflectance values to the peaks between various detectors in Terra and Aqua MODIS band 1. Table 2 lists the differences between detector reflectances and the band-average reflectances for the 10 detectors (D1-D10) of Terra and Aqua band 1 in April 2020. The units are in percentage of band-average reflectance. The differences between different detectors are significant, and larger in Terra B1 than those in Aqua B1. In this study, the long-term monthly D2D differences are calculated in order to evaluate the stability of the D2D differences for selected bands.

**Table 2** The differences between detector reflectances and band-average reflectances for the 10 detectors (D1-D10) of Terra and Aqua band 1 (B1) in April 2020. The units are in percentage of band-average reflectance. Although band 1 has 40 detectors in its native 250 m product, the results in this table are computed using the 1 km aggregated product (10 detectors).

<b>Terra B1</b>	<b>D1</b>	<b>D2</b>	<b>D3</b>	<b>D4</b>	<b>D5</b>	<b>D6</b>	<b>D7</b>	<b>D8</b>	<b>D9</b>	<b>D10</b>
<b>Difference (%)</b>	0.95	0.63	0.20	-0.13	-0.40	-0.56	-0.44	-0.24	-0.15	0.13
<b>Aqua B1</b>	<b>D1</b>	<b>D2</b>	<b>D3</b>	<b>D4</b>	<b>D5</b>	<b>D6</b>	<b>D7</b>	<b>D8</b>	<b>D9</b>	<b>D10</b>
<b>Difference (%)</b>	0.38	0.17	0.09	0.01	-0.05	-0.03	-0.12	-0.17	-0.21	-0.08

### 3. Results and Discussions

To assess the drifts in the D2D differences over DCCs on a monthly basis for Terra and Aqua bands 1, 3-7, and 26, their trends over the mission are examined.

#### 3.1 Stability of D2D Differences at Nadir

Figure 2 shows the long-term trending of monthly D2D differences for Terra and Aqua B1, B3, and B5 over time. The dots represent the derived monthly values, and the solid lines represent a simple linear fit. Noticeable changes in monthly D2D differences over time are seen in Figure 2 and are also quantified in Table 3. For example, the trends of the ratios vary between -0.42% and 0.74% with a span of 1.16% among the 10 detectors for Terra B1, with the edge detectors showing an out-of-family trend with respect to the rest of the detectors. The standard deviations (STDs) in the monthly D2D ratios are no greater than 0.18% for Terra B1, indicating significant increases in D2D differences among the 10 detectors are not primarily caused by the variations in the measurements. Statistically significant changes in D2D differences over time are also shown in Terra B3-B4, B5-B7, and B26. The spans of ratio trends among the 10 detectors are 1.27% for B3, 0.68% for B4, 0.84% for B5 (eight detectors with good quality), 1.59% for B6, 1.88% for B7, and 4.79% for B26. The maximum ratio STD is 0.21% among these bands, indicating that D2D differences increase with time for selected Terra bands. Terra B3 D2D differences have strong seasonal and inter-annual oscillations due to differences in the polarization effects caused by different view geometry between the 10 detectors<sup>16</sup>. The D2D differences are smallest for B3

around year 2008 and increase thereafter. For Terra B5, detectors 2 and 3 are noisy and are therefore not shown here. Detectors 1, 8, and 9 exhibit significant changes over time, but the magnitudes of the drifts for other detectors are less than 0.08%. Figure 2 indicates that the magnitudes of the D2D differences between the 10 detectors in Terra B5 are almost constant over time. As shown in Table 3, for SWIR bands 6, 7, and 26, the trend ranges are noticeably large, which might be caused by the fact that MODIS SWIR bands have an out-of-band (OOB) optical leak issue centered around  $5.3\ \mu\text{m}$  (between the central spectrums of bands 25 and 28), along with electronic crosstalk contamination from thermal bands 20-25. The contamination effects from the thermal bands are large and vary widely over time, especially for Terra SWIR bands. Insufficient correction of OOB optical leak and crosstalk effects on the SWIR bands might be the reason for the large trends of D2D differences for Terra SWIR bands 6, 7, and 26. As noted earlier, the results presented here are linearly scaled from C6.1 L1B; however, in the case of SWIR bands, the crosstalk correction cannot be entirely transferred due to the involvement of the sending signal from the thermal bands when transferring C6.1 L1B reflectances to L1A responses, and further to the updated L1B reflectances as described in Section 2. Future efforts involving reprocessing of the actual L1B with a consistent crosstalk correction will be required to reaffirm this current observation.

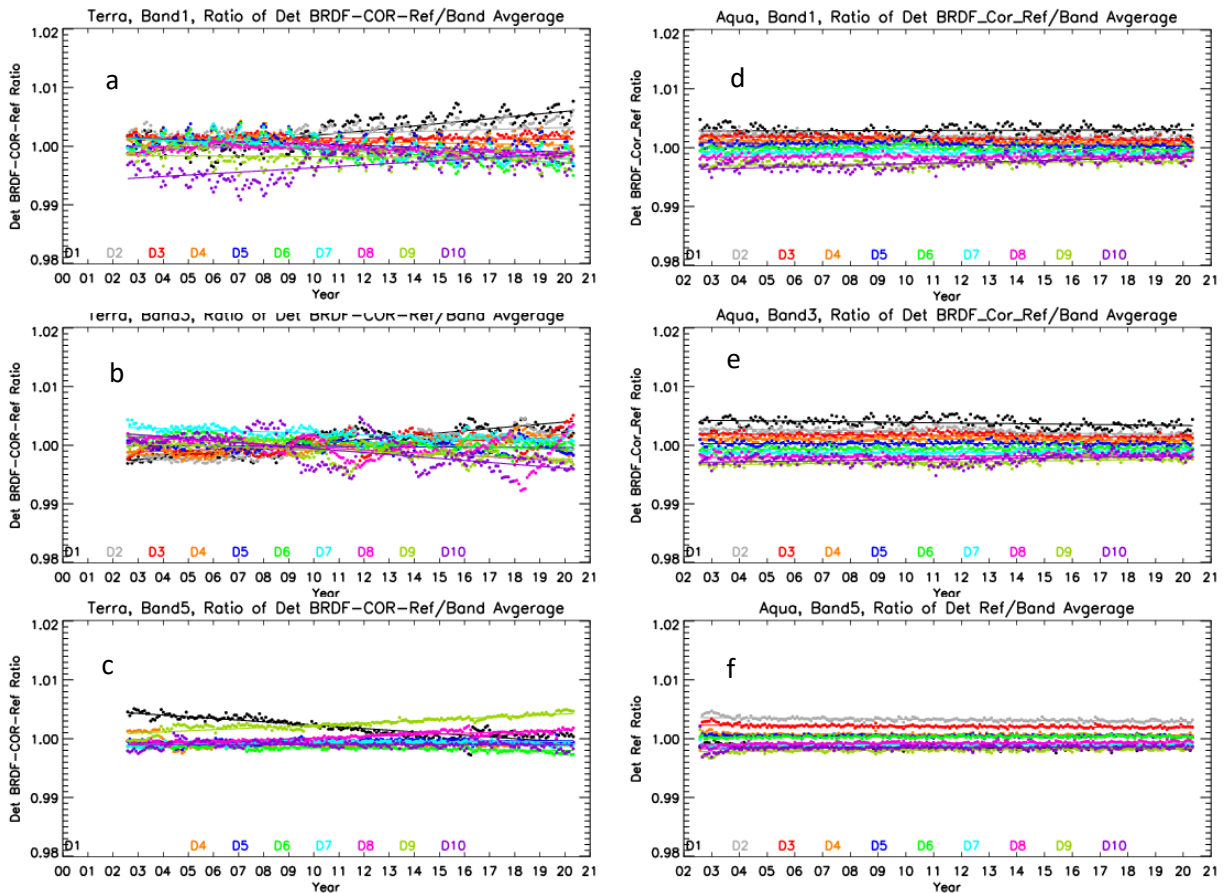


**Figure 2** Monthly ratios of detector reflectance (Ref) to band-average reflectance over DCC samples at nadir for the 10 detectors (product order) of Terra and Aqua bands 1, 3 and 5 from July 2002 through April 2020. For Terra band 5, D2 and D3 are excluded due to the noisy and out-of-family behaviors. The solid lines are the linearly fitted detector reflectance ratios.

**Table 3** The minimum and maximum temporal trends and standard deviations (STDs) in the 10 detectors with good quality in the monthly ratios of detector reflectances to band-average reflectances normalized to their corresponding fitted ratios on July 2002, over DCC samples for select Terra and Aqua RSB at nadir. The units are in percentage of fitted ratios on July, 2002.

<b>Terra DCC</b>	<b>B1</b>	<b>B3</b>	<b>B4</b>	<b>B5</b>	<b>B6</b>	<b>B7</b>	<b>B26</b>
<b>Minimum trend (%)</b>	-0.42	-0.60	-0.27	-0.50	-1.28	-0.85	-1.14
<b>Maximum trend (%)</b>	0.74	0.67	0.41	0.34	0.31	1.03	3.65
<b>Minimum STD (%)</b>	0.06	0.07	0.04	0.03	0.03	0.05	0.07
<b>Maximum STD (%)</b>	0.18	0.21	0.11	0.07	0.10	0.17	0.13
<b>Aqua DCC</b>	<b>B1</b>	<b>B3</b>	<b>B4</b>	<b>B5</b>	<b>B6</b>	<b>B7</b>	<b>B26</b>
<b>Minimum trend (%)</b>	-0.08	-0.10	-0.09	-0.07	////	-0.08	-0.05
<b>Maximum trend (%)</b>	0.21	0.10	0.11	0.06	////	0.09	0.05
<b>Minimum STD (%)</b>	0.04	0.04	0.03	0.02	////	0.03	0.04
<b>Maximum STD (%)</b>	0.08	0.08	0.07	0.04	////	0.07	0.08

For Aqua bands 1, 3, and 5 shown in Figure 2, the magnitude of D2D differences at the beginning of mission are comparable to Terra, but the trends are much more stable in time. For Aqua band 26, the changes in the D2D differences with a maximum of 0.05% in the ratio trends are insignificant over time compared to the maximum of 0.08% in the ratio STDs, as shown in Table 3. The spans of the ratio trends are 0.29% for Aqua B1, 0.20% for B3, 0.20% for B4, 0.13% for B5, and 0.17% for B7, with maximum 0.08% in the ratio STDs. Though the ratio trends are small, the D2D differences in all select Aqua bands become smaller over time. The smaller D2D differences in the Aqua MODIS SWIR bands is an expected phenomenon due to the absence of large electronic crosstalk that is present in the Terra MODIS bands.

### 3.2 Comparisons of the D2D Stability over DCCs and Desert Sites

**Table 4** The minimum and maximum temporal trends and standard deviations (STDs) in the 10 detectors with good quality in the monthly ratios of detector reflectances to band-average reflectances normalized to their corresponding fitted ratios on July, 2002, at Libya-4 desert site for select Terra and Aqua RSB at nadir. The units are in percentage of fitted ratios on July 2002.

<b>Terra Desert</b>	<b>B1</b>	<b>B3</b>	<b>B4</b>	<b>B5</b>	<b>B6</b>
<b>Minimum trend (%)</b>	-0.24	-0.49	-0.23	-0.67	-1.21
<b>Maximum trend (%)</b>	0.49	0.49	0.29	0.33	0.33
<b>Minimum STD (%)</b>	0.18	0.28	0.23	0.15	0.15
<b>Maximum STD (%)</b>	0.30	0.39	0.32	0.26	0.25
<b>Aqua Desert</b>	<b>B1</b>	<b>B3</b>	<b>B4</b>	<b>B5</b>	<b>B6</b>
<b>Minimum trend (%)</b>	-0.22	-0.09	-0.12	-0.09	////
<b>Maximum trend (%)</b>	0.13	0.08	0.13	0.10	////
<b>Minimum STD (%)</b>	0.21	0.27	0.26	0.27	////
<b>Maximum STD (%)</b>	0.30	0.63	0.38	0.45	////

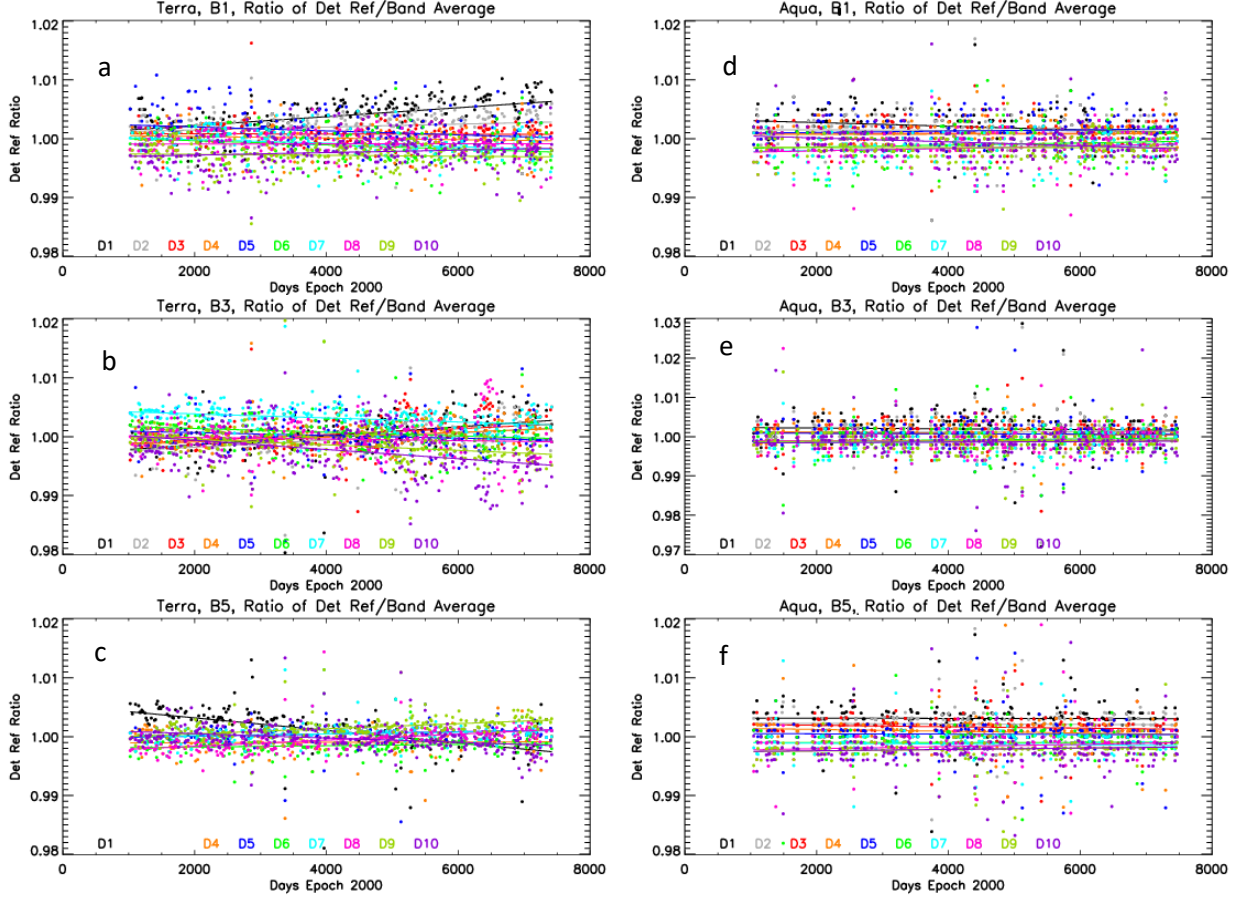


**Figure 3** Monthly ratios of detector reflectance (Ref) to band-average reflectance at Libya-4 desert site for the 10 detectors (product order) of Terra and Aqua bands 1, 3, and 5 from July 2002 through April 2020. For Terra band 5, D2 and D3 are excluded due to the noisy and out-of-family behavior. The solid lines are the linearly fitted detector reflectance ratios.

To perform an independent validation of the D2D difference results obtained from the DCC approach, the results mentioned in subsection 3.1 are compared with those derived over the Libya-4 desert site (28.5°N, 23.4°E), one of the widely used pseudo-invariant desert sites selected to track sensor stability. The primary reason that these desert sites are used is because of their high reflectance and absence of vegetation. The pixel-level reflectance data from near-nadir repeatable orbits every 16 days over a 20 by 20 km window centered at the Libya-4 site are collected. Similar to the DCC approach, the D2D differences at the desert site are derived from an average of pixels for each detector and are normalized to the detector average. B26 is excluded from this analysis because B26 is a water vapor absorption band with very low signal to noise ratio over the desert sites. Band 7 is also excluded in the comparisons because of the large uncertainties in the reflectance at desert sites<sup>17</sup>.

Figure 3 shows the D2D ratio trends for the Libya-4 desert site for the good-quality detectors of select RSBs. The maximum and minimum trends and STDs are listed in Table 4. The trend range of -0.24%–0.49% among the 10 detectors for Terra B1 are significant compared to the uncertainty range of 0.18%–0.30%. In addition, the STDs in the 10 detectors for Terra B1 at the Libya-4 desert site are much higher than those over the DCCs, which indicates that the results over DCCs

are lower noise. This is an expected result given that the desert trends are derived from a single measurement as opposed to an ensemble of DCC pixels. DCCs are highly uniform targets with nearly Lambertian reflectance located at the tropopause level, where the effects of atmospheric absorption are significantly reduced with the exception of stratospheric aerosols and water vapor<sup>11-12</sup>. Both results from DCCs and desert sites show increasing D2D differences in Terra B1, B3-B5, and B6. The trends in Aqua bands are insignificant compared to their large uncertainties.

### 3.3 Stability of D2D Differences over different Frame Zones

For the frames along each EV scan, the AOIs range from 10.5° to 65.5°. The AOIs are around 11° apart in the five frame zones (Z1-Z5) that we divide along each scan. Performance assessments of D2D differences at different AOIs can help improve our understanding of the RVS effects on different detectors. Table 5 lists the differences between detector reflectances and band averages for the 10 detectors of Terra and Aqua band 1 in Z1-Z5 in April 2020. The units are in percentage of band-average reflectance. As shown in Table 3, the STDs for Terra B1 range between 0.06% and 0.18%, and between 0.04% and 0.08% for Aqua B1 among 10 detectors. The differences between detector reflectances and the band averages between Z1-Z5 are close to the STDs. Table 5 indicates that neither AOIs nor RVS effects impact D2D differences significantly.

**Table 5** The differences between detector reflectance to the band-average reflectance for the 10 detectors (D1-D10) of Terra and Aqua band 1 at five frame zones in April 2020. The units are in percentage of band-average reflectance at five zones.

<b>Terra</b>	<b>D1</b>	<b>D2</b>	<b>D3</b>	<b>D4</b>	<b>D5</b>	<b>D6</b>	<b>D7</b>	<b>D8</b>	<b>D9</b>	<b>D10</b>
<b>Zone 1</b>	0.85	0.51	0.14	-0.18	-0.38	-0.48	-0.33	-0.16	-0.08	0.11
<b>Zone 2</b>	0.77	0.62	0.24	-0.06	-0.34	-0.50	-0.30	-0.17	-0.10	-0.16
<b>Zone 3</b>	0.95	0.63	0.20	-0.13	-0.40	-0.56	-0.44	-0.24	-0.15	0.13
<b>Zone 4</b>	0.80	0.65	0.26	-0.08	-0.38	-0.49	-0.31	-0.17	-0.10	-0.17
<b>Zone 5</b>	0.95	0.66	0.24	-0.12	-0.40	-0.52	-0.37	-0.23	-0.20	-0.00
<b>Aqua</b>	<b>D1</b>	<b>D2</b>	<b>D3</b>	<b>D4</b>	<b>D5</b>	<b>D6</b>	<b>D7</b>	<b>D8</b>	<b>D9</b>	<b>D10</b>
<b>Zone 1</b>	0.25	0.17	0.11	0.03	-0.01	-0.01	-0.07	-0.17	-0.25	-0.06
<b>Zone 2</b>	0.17	0.24	0.15	0.13	0.05	-0.02	-0.03	-0.11	-0.19	-0.40
<b>Zone 3</b>	0.38	0.17	0.09	0.01	-0.05	-0.03	-0.12	-0.17	-0.21	-0.08
<b>Zone 4</b>	0.03	0.17	0.16	0.12	0.06	0.01	-0.03	-0.05	-0.12	-0.35
<b>Zone 5</b>	0.18	0.13	0.12	0.10	0.03	-0.02	-0.10	-0.15	-0.20	-0.10

The trends and STDs of the D2D differences in Z1-Z5 are calculated and compared in order to explore if the RVS effects impact the stability of D2D differences at different AOIs. Figures 4 and 5 show the trends and STDs of monthly ratios of detector reflectances to band averages over DCC samples against the 10 detectors of Terra and Aqua bands 1, 3, and 5 from July 2002 through April 2020. The units are the percentage of the linearly fitted ratios in July 2002. The differences of trends and STDs among Z1-Z5 are small for Terra and Aqua B1 and B5. For Terra and Aqua B3, the differences of trends among Z1-Z5 are noticeable. The differences at zones 4 and 5 for Terra B3 are likely due to the seasonal and inter-annual variability caused by polarization effects. Although a detector-dependent RVS has been implemented for Terra band 3, the results below indicate a possible need for improvement in its characterization at all AOIs.



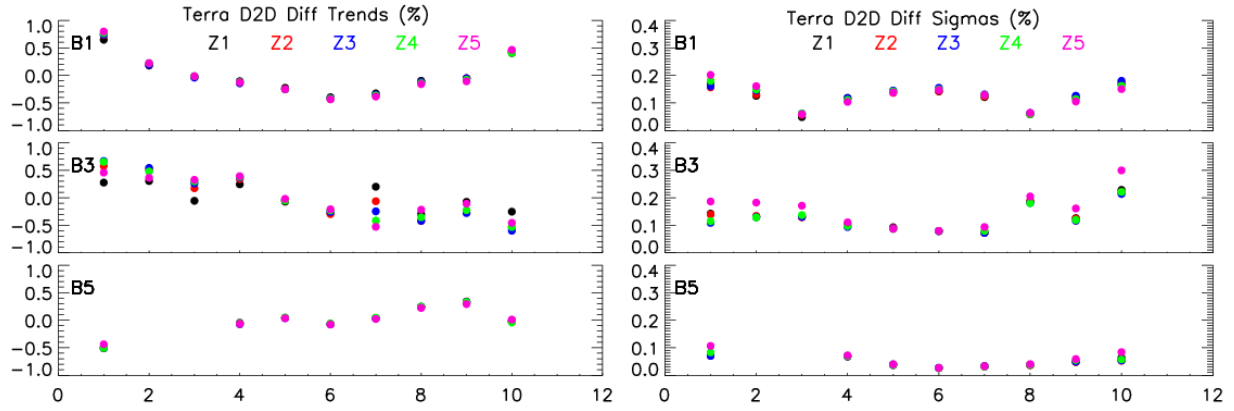


**Figure 4** The trends (Left Panel) and STDs (Right Panel) of monthly ratios of detector reflectance to band-average reflectance over DCC samples for the 10 detectors of Terra bands 1, 3, and 5 from July 2002 through April 2020. Z1-Z5 indicates each frame zone. The units are the percentage of the linearly fitted ratios in July 2002. X-axis is the 10 detectors.

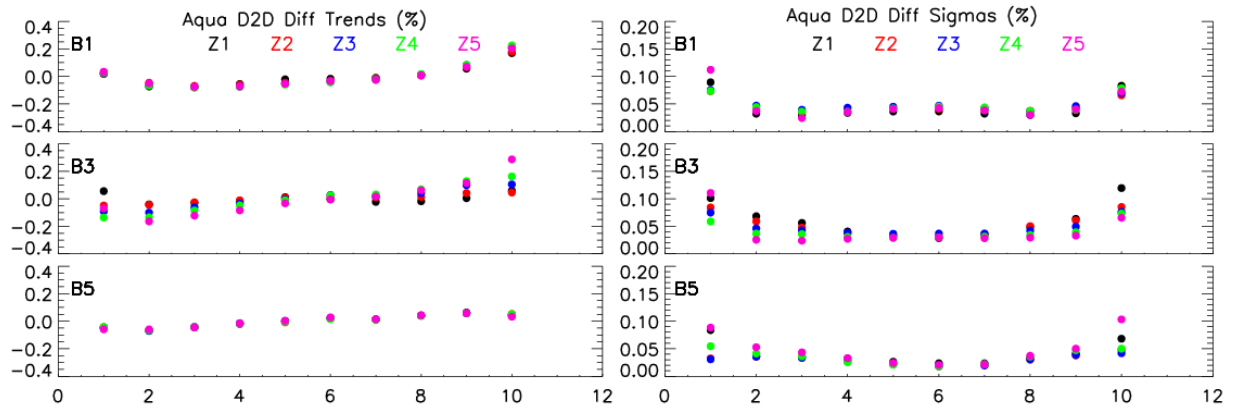


**Figure 5** The trends (Left Panel) and STDs (Right Panel) of monthly ratios of detector reflectance to band-average reflectance over DCC samples over the 10 detectors of Aqua bands 1, 3, and 5 from July 2002 through April 2020. Z1-Z5 mean zones 1-5. The units are the percentage of the linearly fitted ratios in July, 2002. X-axis is the 10 detectors.

## 4. Conclusions

In this work, DCCs are used to assess the D2D differences for MODIS RSBs. Results indicate that residual D2D differences exist in Terra and Aqua RSBs 1, 3-7, and 26. Furthermore, D2D difference results show noticeable increases over time for Terra bands 1, 3-5, and significant increases for Terra SWIR bands 6, 7, and 26, which can induce noticeable striping and higher uncertainties in the downstream scientific products. The large increases in Terra SWIR bands 6, 7, and 26 are likely due to the inadequate correction of the contaminations caused by OOB optical leak and crosstalk from thermal bands, an issue that is expected to show improvement in a future L1B reprocess. The D2D differences are more stable in the Aqua bands over time, with small decreases in the magnitudes of D2D differences except for Aqua band 26. The independent results at the Libya-4 desert site are consistent with those over DCCs, confirming the increases in D2D

difference for Terra bands and the decreases in Aqua bands over time. Since the desert measurements have larger uncertainties in D2D reflectances than those over DCCs, the DCC approach is more reliable than using the desert site. The D2D differences also exhibit an AOI-dependency in Terra bands 3 and 4, as well as Aqua band 3, therefore suggesting a need for improvement in the detector-dependent RVS algorithm. The impacts from AOIs are small for Terra and Aqua bands 1 and SWIR bands, and Aqua band 4.

### **Acknowledgments:**

The authors would like to thank Sarah Henderson for her help to review this manuscript.

### **5. References**

1. Xiong, X., M. D. King, V. Salomonson, W. Barnes, B. N. Wenny, A. Angal, A. Wu, S. Madhavan, and D. Link, "Moderate Resolution Imaging Spectroradiometer on Terra and Aqua Missions", John Wiley & Sons, Ltd, vol. 9781118945179, pp. 53-89, 2015.
2. Xiong, X., A. Angal, J. Sun, J. Choi, and E. Johnson, "On-orbit performance of MODIS Solar Diffuser Stability Monitor", *Journal of Applied Remote Sensing*, vol. 8, pp. 083514-1-14, 2014.
3. Sun, J., X. Xiong, W. Barnes, and B. Guenther, "MODIS Reflective Solar Bands On-Orbit Lunar Calibration", *IEEE Trans. Geosci. Remote Sens.*, vol. 45, issue 7, pp. 2383-2393, 2007.
4. X. Xiong, J. Sun, X. Xie, W. L. Barnes, and V. V. Salomonson, "On-orbit calibration and performance of Aqua MODIS reflective solar bands", *IEEE Trans. Geosci. Remote Sens.*, vol. 48, no. 1, pp. 535–546, Jan. 2010.
5. Angal, A., J. Sun, X. Geng, M. Chu, and X. Xiong, "Assessment of the MODIS RSB detector differences using earth-view targets ", *Proc. SPIE 8866, Earth Observing Systems XVIII*, 88661T, 2013.
6. Di Bisceglie, M., R. Episcopo, C. Galdi, and S.L. Ullo, "Destriping MODIS data using overlapping field-of-view method", *IEEE Trans. Geosci. Remote Sens.*, 47(2), 637–651, 2009.
7. Bouali, M., and S. Ladjal, "Toward optimal destriping of MODIS data using a unidirectional variational model", *IEEE Trans. Geosci. Remote Sens.*, 49(8), 2924–2935, 2011.
8. Li, Y., Angal, A., Wu, A., Geng, X., Link, D. and Xiong, X.J., "Calibration improvements in the detector-to-detector differences for the MODIS ocean color bands", *Proc. SPIE 9972, Earth Observing Systems XXI*, 99721V, 2016.
9. Chang, T., X. (J.) Xiong, A. Angal, and Q. Mu, "Assessment of MODIS RSB detector uniformity using deep convective clouds", *J. Geophys. Res. Atmos.*, 121, 4783–4796, 2016.
10. Mu, Q., A. Wu, X. Xiong, A. Angal, "Assessment of SNPP VIIRS RSB detector-to-detector differences using deep convective clouds and deserts", *J. Appl. Remote Sens.* 14(1), 018503, 2020.
11. Doelling, D.R., L. Nguyen, P. Minnis, "On the use of deep convective clouds to calibrate AVHRR data", *Proc. SPIE 5542*, 281–289, 2004.
12. Mu, Q., Wu, A., Xiong, X., Doelling, D.R., Angal, A., Chang, T. and Bhatt, R., "Optimization of a deep convective cloud technique in evaluating the long-term

- radiometric stability of MODIS reflective solar bands”, *Remote Sensing*, 9(6), p.535, 2017.
13. Doelling, D.R., Morstad, D.L., Bhatt, R. and Scarino, B. “Algorithm theoretical basis document (ATBD) for deep convective cloud (DCC) technique of calibrating GEO sensors with Aqua-MODIS for GSICS”, GSICS, World Meteorological Organization, Geneva, 2011.
  14. Xiong, X., Angal, A., and Li, Y., “Improvements in the on-orbit calibration of the Terra MODIS short-wave infrared spectral bands,” *Proc. SPIE* 10781, 107811C–1–8, 2018.
  15. Doelling, D. R., D. Morstad, B. R. Scarino, R. Bhatt, and A. Gopalan, “The characterization of deep convective clouds as an invariant calibration target and as a visible calibration technique”, *IEEE Trans. Geosci. Remote Sens.*, 51, 1147–1159, 2013.
  16. Sun, J.Q. and Xiong, X., “MODIS polarization-sensitivity analysis”, *IEEE transactions on geoscience and remote sensing*, 45(9), pp.2875-2885, 2007.
  17. Wang, L., Qu, J.J., Hao, X. and Zhu, Q., “Sensitivity studies of the moisture effects on MODIS SWIR reflectance and vegetation water indices”, *International Journal of Remote Sensing*, 29(24), pp.7065-7075, 2008.